

# Magic mass ratios of complete energy-momentum transfer in one-dimensional elastic three-body collisions

June-Haak Ee and Jungil Lee\*

*Department of Physics, Korea University, Seoul 136-713, Korea*

(Dated: January 19, 2017)

## Abstract

We consider the one-dimensional scattering of two identical blocks of mass  $M$  that exchange energy and momentum via elastic collisions with an intermediary ball of mass  $m = \alpha M$ . Initially, one block is incident upon the ball with the other block at rest. For  $\alpha < 1$ , the three objects will make multiple collisions with one another. In our analysis, we construct a Euclidean vector  $\mathbf{V}_n$  whose components are proportional to the velocities of the objects. Energy-momentum conservation then requires a covariant recurrence relation for  $\mathbf{V}_n$  that transforms like a pure rotation in three dimensions. The analytic solutions of the terminal velocities result in a remarkable prediction for values of  $\alpha$ , in cases where the initial energy and momentum of the incident block are completely transferred to the scattered block. We call these values for  $\alpha$  “magic mass ratios.”

## I. INTRODUCTION

If two identical particles make a head-on collision, they exchange energy and momentum in any reference frame.<sup>1</sup> In a frame where the target is initially at rest, the target can acquire all of the energy and momentum of the incident object, causing the incident object to come to rest. Such a complete energy-momentum transfer, however, is rarely observed in many-body collisions. A specific example is Newton's cradle, which consists of a series of identical pendula that are aligned on a horizontal level. Newton's cradle can be understood as a series of head-on collisions of two identical objects where small gaps between each pair of adjacent pendula are assumed.<sup>2-4</sup>

Although this small-gap model for Newton's cradle explains the observations, the model fails if some of the adjacent pendula are in contact with each other, in which case the process cannot be decomposed into a series of two-body collisions. The reason for this failure is that the constraints of energy-momentum conservation are not enough to determine the final velocities. Additional conditions, such as force laws between objects, are required to obtain a unique solution of the problem. Various studies have been carried out to find an appropriate force law that governs the actual motions of the pendula. For example, the contact Hertz force of the form  $F = -kx^{3/2}$  is such a phenomenological model.<sup>4-8</sup> Further applications of the contact Hertz force to various collision problems can be found in Refs. 9–13.

In a previous work, we studied the bouncing of a block against a rigid wall through one-dimensional multiple elastic collisions with a ball sandwiched between them.<sup>14</sup> Based on the assumption that each collision is instantaneous, as in the small-gap model, we obtained the unique analytic solutions to the complete trajectories of the block and the ball. By taking the continuum limit of the block trajectory, we have shown that the effective force carried by the ball is proportional to  $1/r^3$ , where  $r$  is the distance between the block and the wall. This is consistent with previous results based on the differential equation that can be derived by taking the continuum limit of energy-momentum conservation.<sup>15,16</sup>

In this paper, we generalize the model system of Ref. 14 to a simple three-body system. Here we consider the scattering of two identical blocks of mass  $M$  through multiple elastic collisions with a ball of mass  $m = \alpha M$  sandwiched between the blocks. As shown in Fig. 1, the ball  $C$  and the target block  $B$  are initially placed at locations  $x = 0$  and  $L$ , respectively, and the block  $A$  is incident to the target with initial velocity  $V$ . If  $\alpha < 1$ , then the system

experiences multiple collisions that can be understood as a series of two-body collisions and, therefore, the velocities of all objects are uniquely determined. To aid in visualizing the discussion below, the reader is encouraged to view the animation of a series of such collisions in the online video linked to Fig. 6.

In our analysis, we construct a Euclidean vector whose components are proportional to the velocities of the objects. With such, the energy-momentum conservation constraints reduce to a pure rotational transformation under which the magnitude of the Euclidean vector is invariant. This covariant approach is equivalent to the billiard-ball mapping approach in Refs. 17–21, that reformulates the collision problem into a problem of projective geometry. While we were interested in the trajectories of the objects and the effective force in Ref. 14, here we focus on the energy-momentum transfer from the incident block  $A$  to the scattered block  $B$ . As a result, we find all possible values for the *magic mass ratios*  $\alpha = \alpha^{\text{magic}}$  at which the energy and momentum of the incident block are completely transferred to the scattered block.

The chain collisions of multiple pendula in series have been studied previously by Hart *et al.*<sup>2</sup> and by Kerwin.<sup>3</sup> However, the pendula studied in these references are arranged in mass order so that the complete energy-momentum transfer from the incident pendulum to the target pendulum at the other end is achieved only if all of the pendula are of equal mass, as in Newton’s cradle. Redner considered a similar system consisting of two identical cannonballs approaching an initially stationary ping-pong ball.<sup>21</sup> In that study, the author focuses mainly on deriving a simple relation between the elastic collision and a corresponding billiard system, which helps to determine the total number of collisions of the system. Thus, to our best knowledge, the derivation of all possible magic mass ratios  $\alpha^{\text{magic}}$  for which complete energy-momentum transfer is realized is new.

This paper is organized as follows. In Sec. II, we describe the model system and provide the definitions of kinematic variables that we use throughout the paper. In Sec. III, we construct the covariant recurrence relation for the velocity sequences of the objects and compare this approach with the billiard-ball mapping. Our results for the terminal velocities and kinematic variables including the magic mass ratios are given in Sec. IV. Finally, we offer our conclusions in Sec. V and provide some technical details in the Appendices.

## II. MODEL, TERMINOLOGY, AND CONJECTURES

In this section, we describe the model system and define kinematic variables that we use throughout the paper. We also discuss some conjectures regarding the relationship among special values for mass ratios.

### A. Model

As shown in Fig. 1, the model system consists of two identical blocks  $A$  and  $B$ , each of mass  $M$ , and a ball  $C$  with mass  $m = \alpha M$ , all aligned on the  $x$ -axis. Initially,  $C$  and  $B$  are at rest at  $x = 0$  and  $L$ , respectively, and block  $A$  is at  $x < 0$  and moving toward ball  $C$  with speed  $V$ . At time  $t = 0$ , block  $A$  collides with the ball. We assume that all of the collisions are (completely) elastic and ignore friction. If the mass of  $C$  is equal to or larger than the mass of the blocks ( $\alpha \geq 1$ ), then  $C$  will collide with each block only once. But if  $C$  is less massive than the blocks ( $\alpha < 1$ ), then it moves back and forth to make multiple collisions with the blocks. In either case, because each collision is governed by a repulsive force,  $A$  must decelerate and  $B$  must accelerate. In this paper, we are interested in the situation where  $A$  and  $B$  interact through multiple elastic collisions with  $C$  (i.e.  $\alpha < 1$ ).

### B. Terminology

We use an integer  $n$  to identify the sequence of collisions of the ball with a block. We denote by  $P_n$  the  $n$ th collision point between objects  $A$  and  $C$ , and by  $Q_n$  the  $n$ th collision point between objects  $B$  and  $C$ . The velocities of the three objects are defined as follows:  $a_n$  and  $c_n$  are the velocities of  $A$  and  $C$ , respectively, immediately after the collision at  $P_n$ . Likewise,  $b_n$  and  $c'_n$  are the velocities of  $B$  and  $C$ , respectively, immediately after the collision at  $Q_n$ . During the ball's motion from  $P_n$  to  $Q_n$ , the velocity of  $C$  is fixed at  $c_n$ ; between  $Q_n$  and  $P_{n+1}$ , the velocity of  $C$  is  $c'_n$ .

Because  $\alpha$  is a finite number, the total number of collisions between  $C$  and a block is also finite. We call  $N_A$  and  $N_B$  the total number of collisions between blocks  $A$  and  $B$  and the ball, respectively. After these final collisions, blocks  $A$  and  $B$  reach their terminal velocities  $a_t = a_{N_A}$  and  $b_t = b_{N_B}$ , respectively. Conservation of (linear) momentum determines the terminal velocity of  $C$  as  $c_t = (V - a_t - b_t)/\alpha$ .

If  $\alpha$  is decreased, then  $N_A$  and  $N_B$  will increase by unity at certain values of  $\alpha$ . We call  $\alpha_k$  and  $\beta_k$  the  $k$ th *threshold mass ratios* of  $A$  and  $B$ , which are the minimum values for  $\alpha$  with  $N_A = k$  and  $N_B = k$  for  $k \geq 1$ , respectively. Therefore, the values for  $N_A$  and  $N_B$  are determined by the mass ratio  $\alpha$  as

$$N_A = k \quad \text{for} \quad \alpha_k \leq \alpha < \alpha_{k-1} \quad (1)$$

and

$$N_B = k \quad \text{for} \quad \beta_k \leq \alpha < \beta_{k-1}, \quad (2)$$

where we set  $\alpha_0 = \infty$  and  $\beta_0 = \infty$ .

In a many-body, fixed-target collision, it is not easy to determine the masses so that the kinetic energy of the incident particle is completely transferred to a single scattered particle (leaving the incident particle at rest). However, in some situations, such as with Newton's cradle or the situation we consider here, it is possible to solve for the masses. There are two classes of critical mass ratios, the *magic mass ratio* and the *deficient mass ratio*. We denote by  $\alpha_k^{\text{magic}}$  the  $k$ th magic mass ratio at which both  $A$  and  $C$  stop moving and  $B$  carries the complete energy and momentum of the incident block. Between any two consecutive magic mass ratios  $\alpha_k^{\text{magic}}$  and  $\alpha_{k+1}^{\text{magic}}$ , there will be a mass ratio for which the energy-momentum transfer is the least efficient. We call this value the  $k$ th deficient mass ratio  $\alpha_k^{\text{deficient}}$ .

### C. Conjectures $\alpha_k^{\text{magic}} = \alpha_k$ and $\alpha_k^{\text{deficient}} = \beta_k$

Before working through the details, we can make an educated guess that  $\alpha_k^{\text{magic}} = \alpha_k$ . Let us suppose that there exists  $\alpha_k^{\text{magic}}$  where the scattered block takes all of the kinetic energy of the incident block. Thus, the momentum transfer from block  $A$  to block  $B$  is at a maximum. In this case, both  $A$  and  $C$  must remain at rest after the final collision. Such a configuration is feasible only if  $A$  stops at  $P_k$  ( $a_k = 0$ ),  $C$  stops at  $Q_k$  ( $c'_k = 0$ ), and  $B$  carries the initial velocity of the incident block  $A$  ( $b_k = V$ ). In fact, these conditions require<sup>22</sup>  $c_k = 2V/(1 + \alpha_k^{\text{magic}})$ , and also lead to  $N_A = N_B = k$ . Next, we take  $\alpha = \alpha_k^{\text{magic}} - \varepsilon$ , which is infinitesimally smaller than  $\alpha_k^{\text{magic}}$  ( $\varepsilon \rightarrow 0^+$ ). Then the momentum transfer between  $A$  and  $B$  that is mediated by  $C$  must be infinitesimally less than when  $\alpha = \alpha_k^{\text{magic}}$ , and the ball must carry a surplus of energy after the last collision, and this will lead to an additional collision with block  $A$ .

Similarly, we might guess that at  $\alpha = \beta_k$  the final kinetic energy of the ball reaches a local maximum. We shall find that these conjectures are in fact true:  $\alpha_k^{\text{magic}} = \alpha_k$  and  $\alpha_k^{\text{deficient}} = \beta_k$  for all  $k$ .

### III. ANALYTIC COMPUTATION IN COVARIANT APPROACH

In this section, we use energy and momentum conservation to develop a recurrence relation for a column vector  $\mathbf{V}_n$  constructed from the velocities of blocks  $A$  and  $B$  and ball  $C$ . This approach is compared with an alternative method—the billiard-ball mapping of Redner—that can be applied to a similar problem.<sup>21</sup>

#### A. Construction of a Euclidean vector in terms of velocities

It is convenient to define the column-vector sequence  $\mathbf{V}_n$  as

$$\mathbf{V}_n \equiv \begin{pmatrix} a_n \\ b_n \\ \sqrt{\alpha}c'_n \end{pmatrix}, \quad (3)$$

where the scaling factor  $\sqrt{\alpha}$  of the third component is introduced to simplify the following analyses. The magnitude of the three-dimensional Euclidean vector  $\mathbf{V}_n$  is defined by  $|\mathbf{V}_n| \equiv \sqrt{\mathbf{V}_n^2}$ , where  $\mathbf{V}_n^2 \equiv (V_n)_1^2 + (V_n)_2^2 + (V_n)_3^2$  and  $(V_n)_i$  is the  $i$ th Cartesian component of  $\mathbf{V}_n$ ; namely,  $(V_n)_1 = a_n$ ,  $(V_n)_2 = b_n$ , and  $(V_n)_3 = \sqrt{\alpha}c'_n$ . We shall see in the following section that energy conservation forces  $|\mathbf{V}_n|$  to be independent of  $n$  and the transformation of  $\mathbf{V}_{n-1}$  into  $\mathbf{V}_n$  is linear. This covariant transformation can be formulated by making use of an orthogonal matrix  $\mathcal{O}$ . (Some useful properties of orthogonal matrices are summarized in Appendix A).

#### B. Covariant recurrence relation for $\mathbf{V}_n$

The collision at  $P_n$  transforms the velocities  $a_{n-1}$  and  $c'_{n-1}$  into  $a_n$  and  $c_n$ , respectively. The collision at  $Q_n$  transforms the velocities  $b_{n-1}$  and  $c_n$  into  $b_n$  and  $c'_n$ , respectively. Con-

servation of momentum and kinetic energy in the collisions at  $P_n$  and  $Q_n$  requires

$$a_{n-1} + \alpha c'_{n-1} = a_n + \alpha c_n, \quad (4)$$

$$a_{n-1}^2 + (\sqrt{\alpha} c'_{n-1})^2 = a_n^2 + (\sqrt{\alpha} c_n)^2, \quad (5)$$

$$b_{n-1} + \alpha c_n = b_n + \alpha c'_n, \quad (6)$$

and

$$b_{n-1}^2 + (\sqrt{\alpha} c_n)^2 = b_n^2 + (\sqrt{\alpha} c'_n)^2. \quad (7)$$

The sum of Eqs. (5) and (7) yields the energy-conservation constraint under the  $n$ th cycle of collisions at  $P_n$  and  $Q_n$ :

$$a_{n-1}^2 + b_{n-1}^2 + (\sqrt{\alpha} c'_{n-1})^2 = a_n^2 + b_n^2 + (\sqrt{\alpha} c'_n)^2. \quad (8)$$

By coupling to the constraint (4), we can reduce Eq. (5) for the collision at  $P_n$  into a linear form. In a similar manner, Eq. (7) for the collision at  $Q_n$  also reduces into a linear form. The result is

$$a_{n-1} - c'_{n-1} = -a_n + c_n, \quad (9)$$

$$b_{n-1} - c_n = -b_n + c'_n. \quad (10)$$

The reduction in Eqs. (9) and (10) is allowed as long as  $a_{n-1} \neq a_n$ ,  $b_{n-1} \neq b_n$ ,  $c'_{n-1} \neq c_n$ , and  $c_n \neq c'_n$ . These requirements are always satisfied because every collision changes the velocity of each participant.

If we now employ the notation for the vector  $\mathbf{V}_n$  defined in Eq. (3), we find that Eq. (8) can be expressed as

$$\mathbf{V}_n^2 = \mathbf{V}_{n-1}^2. \quad (11)$$

Similarly, after eliminating  $c_n$  from Eqs. (4), (6), (9), and (10), we end up with three equations that can be written as

$$\mathbf{V}_n = \Lambda \mathbf{V}_{n-1}, \quad (12)$$

where  $\Lambda$  is a  $3 \times 3$  matrix that depends only on  $\alpha$ . By applying the recurrence relations (11) and (12) repeatedly, we find that the length of vector  $\mathbf{V}_n$  is invariant ( $\mathbf{V}_n^2 = \mathbf{V}_0^2$ ) and

$$\mathbf{V}_n = \Lambda^n \mathbf{V}_0, \quad (13)$$

where  $\mathbf{V}_0 = (V \ 0 \ 0)^T$ .

The constraints in Eqs. (11) and (12) are equivalent to the covariant transformation rule for a Euclidean vector  $\mathbf{V} \rightarrow \mathbf{V}' = \mathcal{O}\mathbf{V}$  that preserves its magnitude  $|\mathbf{V}'| = |\mathbf{V}|$ . In a Cartesian coordinate system, the magnitude is defined by  $|\mathbf{V}| = (\mathbf{V} \cdot \mathbf{V})^{1/2} = (\sum_i V_i^2)^{1/2}$ , where  $V_i$  is the  $i$ th Cartesian coordinate of  $\mathbf{V}$ . Such a transformation also preserves any scalar product of such vectors  $\mathbf{V} \cdot \mathbf{W} = \sum_{i,j} V_i \delta_{ij} W_j = \sum_i V_i W_i$ , where the Kronecker delta  $\delta_{ij}$  is the *metric tensor* of the Euclidean space. The invariance of the scalar product under this transformation requires that the matrix  $\mathcal{O}$  must be orthogonal; stated another way, the inverse of  $\mathcal{O}$  is the same as its transpose:  $\mathcal{O}^{-1} = \mathcal{O}^T$ . In addition, for any orthogonal matrix  $\mathcal{O}$ ,  $\det[\mathcal{O}] = \pm 1$ . An orthogonal matrix with  $\det[\mathcal{O}] = +1$  can be expressed as a pure rotation, while an orthogonal matrix with  $\det[\mathcal{O}] = -1$  can be expressed as either a reflection or the product of a pure rotation and a reflection. We call the formulation in Eqs. (11) and (12) the *covariant* approach.

By generalizing the method in Ref. 14 for two-body multiple collisions against a rigid wall, we develop a systematic way to determine  $\Lambda$  and  $\Lambda^n$ . As is stated in Appendix A, the orthogonal matrix  $\Lambda$  represents a pure rotation about an axis  $\hat{n}$  by a finite angle  $\psi$  in three dimensions. Thus, according to Eq. (13),  $\mathbf{V}_n$  can be obtained by rotating  $\mathbf{V}_0$  about the same axis  $\hat{n}$  by  $n\psi$ . Because  $\alpha$  is the only variable that involves the transformation of  $\mathbf{V}_n$ , both  $\hat{n}$  and  $\psi$  depend only on  $\alpha$ .

### C. Comparison with billiard-ball mapping

In principle, the covariant approach summarized in Eqs. (11) and (12) is equivalent to the billiard-ball mapping described by Redner in Ref. 21. Redner also rescaled the velocity by multiplying the square root of its mass as we did in constructing the Euclidean vector  $\mathbf{V}_n$ . The crucial constraint in Redner's billiard-ball mapping is that the scalar product  $(\sqrt{m_1}, \sqrt{m_2}) \cdot (w_1, w_2)$  is conserved. Here,  $m_i$  is the mass of the  $i$ th particle in a two-body collision and  $w_i = \sqrt{m_i} v_i$  is the rescaled velocity  $v_i$  of particle  $i$ :  $(\sqrt{m_1}, \sqrt{m_2}) \cdot (w_1, w_2) = (\sqrt{m_1}, \sqrt{m_2}) \cdot (w'_1, w'_2)$ , where the primed variable is used for a particle after a collision. This constraint originates from the momentum conservation law in Eqs. (4) and (6) and is equivalent to the covariant transformation rule of Eq. (12). Geometrically, the conservation of the projection of the vector  $(w_1, w_2)$  onto the vector  $(\sqrt{m_1}, \sqrt{m_2})$  implies that the transformation of  $(w_1, w_2)$  into  $(w'_1, w'_2)$  must be related to a

rotation about an axis parallel to  $(\sqrt{m_1}, \sqrt{m_2})$  and/or a reflection of the component perpendicular to  $(\sqrt{m_1}, \sqrt{m_2})$ . Therefore, the covariant approach must be equivalent to the billiard-ball mapping approach. Redner then reformulated the problem into a problem of projective geometry.

The merit of the covariant approach is that the corresponding computation techniques are available in standard textbooks on classical mechanics or mathematical physics, such as Refs. 23 and 24. An extension of the covariant approach into a relativistic collision is even feasible at the level of undergraduate physics majors. A generalization of the billiard-ball mapping of a projective geometry into that in the Minkowski space needs additional work.

#### D. Determination of $\Lambda$

The recurrence relations (11) and (12) represents the transformation of the velocities after two collisions at  $P_n$  and  $Q_n$ . Because each collision is elastic, there exist orthogonal (*collision*) matrices— $\Gamma_A$  for the collision at  $P_n$  and  $\Gamma_B$  for that at  $Q_n$ —that preserve the magnitude of  $\mathbf{V}_n$ . In this case,  $\Lambda$  must be expressed as

$$\Lambda = \Gamma_B \Gamma_A. \quad (14)$$

Here,  $B$  does not participate in the collision at  $P_n$  and  $A$  is independent of the collision at  $Q_n$  so that  $\Gamma_A$  and  $\Gamma_B$  maintain the velocities of  $B$  and  $A$ , respectively. Thus,  $\Gamma_A$  and  $\Gamma_B$  are intrinsically two-dimensional linear transformations. The matrix  $\Gamma_i$  for the elastic collision of one-dimensional two-body scattering has the determinant  $-1$  (see, for example, Ref. 14). Therefore, each collision matrix can be parametrized by the product of a pure rotation and a reflection so that  $\det[\Gamma_A] = \det[\Gamma_B] = -1$ . By making use of the properties of  $3 \times 3$  orthogonal matrices summarized in Appendix A, we find the useful parametrizations

$$\Gamma_A = \lambda_2(-\theta) \mathbb{P}_3 \quad (15)$$

and

$$\Gamma_B = \lambda_1(\theta) \mathbb{P}_3, \quad (16)$$

where  $\lambda_i(\theta)$  are rotation matrices about the  $i$ th Cartesian axis,  $\mathbb{P}_3 = \text{diag}[1, 1, -1]$  is a reflection matrix, and  $\theta$  is given by

$$\theta = 2 \arctan \sqrt{\alpha}. \quad (17)$$

We then find the explicit form of the matrix  $\Lambda$  as

$$\Lambda = \begin{pmatrix} \frac{1-\alpha}{1+\alpha} & 0 & \frac{2\sqrt{\alpha}}{1+\alpha} \\ \frac{4\alpha}{(1+\alpha)^2} & \frac{1-\alpha}{1+\alpha} & -\frac{2(1-\alpha)\sqrt{\alpha}}{(1+\alpha)^2} \\ -\frac{2(1-\alpha)\sqrt{\alpha}}{(1+\alpha)^2} & \frac{2\sqrt{\alpha}}{1+\alpha} & \frac{(1-\alpha)^2}{(1+\alpha)^2} \end{pmatrix}. \quad (18)$$

An explicit computation shows that  $\Lambda^T = \Lambda^{-1}$  (i.e.  $\Lambda$  is orthogonal). A detailed procedure to compute  $\Lambda$  is given in Appendix B.

### E. Computation of $\Lambda^n$

Direct computation of  $\Lambda^n$  by repeated multiplications of  $\Lambda$  is not trivial. However, the analysis can be greatly simplified if we make use of the identity in Eq. (14) and the parametrization  $\lambda_{\hat{n}}(\phi) = R \lambda_3(\phi) R^T$ , where  $R$  is an orthogonal matrix (see Appendix A).

Given that  $\det[\Gamma_A] = \det[\Gamma_B] = -1$ , we know that  $\det[\Lambda] = \det[\Gamma_A]\det[\Gamma_B] = +1$ . Therefore,  $\Lambda$  can be parametrized by a pure rotation  $\Lambda = R \lambda_3(\psi) R^T$ , where the angle of rotation  $\psi$  must be a function of  $\alpha$  only. Because  $R$  is orthogonal, it is straightforward to find that

$$\Lambda^n = R \lambda_3(n\psi) R^T, \quad (19)$$

where we have used the fact that  $[\lambda_3(\psi)]^n = \lambda_3(n\psi)$ . According to the expression for  $\Lambda^n$  in Eq. (19), it is manifest that an additional cycle of collisions at  $P_n$  and  $Q_n$  merely increases the phase by a constant  $\psi$  about the same axis of rotation.

A detailed derivation of  $\Lambda^n$  is provided in Appendix C; here we simply quote the  $\alpha$  dependence of  $\psi$  and  $R$ :

$$\psi = 2 \arctan \sqrt{\alpha(2+\alpha)} \quad (20)$$

and

$$R = \begin{pmatrix} -\frac{1}{\sqrt{2}} & -\sqrt{\frac{\alpha}{2(2+\alpha)}} & \frac{1}{\sqrt{2+\alpha}} \\ \frac{1}{\sqrt{2}} & -\sqrt{\frac{\alpha}{2(2+\alpha)}} & \frac{1}{\sqrt{2+\alpha}} \\ 0 & \sqrt{\frac{2}{2+\alpha}} & \frac{\sqrt{\alpha}}{\sqrt{2+\alpha}} \end{pmatrix}. \quad (21)$$

As with  $\Lambda$ , an explicit computation confirms that  $R$  is orthogonal ( $R^T = R^{-1}$ ). Having found  $R$ , we know that the third column of  $R$  is the unit vector  $\hat{n}$  that is parallel to the axis of rotation for  $\Lambda$ . We find that  $\hat{n}$  is parallel to  $(\sqrt{M_A} \sqrt{M_B} \sqrt{M_C})^T$ , where  $M_i$  is the mass of  $i = A, B$ , and  $C$ , supporting our earlier argument that the covariant approach is equivalent to the billiard-ball mapping approach.

#### IV. RESULTS

In this section, we find the general terms of the velocity sequences  $a_n$ ,  $b_n$ ,  $c_n$ , and  $c'_n$  by solving the recurrence relation for  $\mathbf{V}_n$ . By making use of these analytic solutions, we calculate  $N_A$  and  $N_B$ , and obtain the threshold mass ratios  $\alpha_k$  and  $\beta_k$ . We then determine the terminal velocities of the objects and show that the magic mass ratio  $\alpha_k^{\text{magic}}$  and the deficient mass ratio  $\alpha_k^{\text{deficient}}$  are identical to the threshold mass ratios  $\alpha_k$  and  $\beta_k$ , respectively. Lastly, we discuss possible modifications of our predictions for inelastic collisions.

Substituting the initial condition  $\mathbf{V}_0 = (V \ 0 \ 0)^T$  and  $\Lambda^n$  in Eq. (19) into Eq. (13), we can determine  $\mathbf{V}_n$ . The value of  $c_n$  can be computed by substituting  $a_{n-1}$ ,  $a_n$ , and  $c'_{n-1}$  into Eq. (4). The general terms for the velocity sequences are obtained as

$$a_n = V_{\text{CM}} \left\{ 1 + \frac{\cos(n\psi)}{\cos(\psi/2)} \right\}, \quad (22)$$

$$b_n = V_{\text{CM}} \left\{ 1 - \frac{\cos[(n + \frac{1}{2})\psi]}{\cos(\psi/2)} \right\}, \quad (23)$$

$$c_n = V_{\text{CM}} \left\{ 1 + \frac{\sin[(n - \frac{1}{4})\psi]}{\sin(\psi/4)} \right\}, \quad (24)$$

and

$$c'_n = V_{\text{CM}} \left\{ 1 - \frac{\sin[(n + \frac{1}{4})\psi]}{\sin(\psi/4)} \right\}, \quad (25)$$

where  $V_{\text{CM}}$  is the velocity of the center-of-mass, given by

$$V_{\text{CM}} = \frac{V}{2 + \alpha} = \frac{V \cos(\psi/2)}{1 + \cos(\psi/2)}. \quad (26)$$

Note that  $(m + 2M)V_{\text{CM}} = MV$  is the total linear momentum of the system. If we make a Galilean transformation into the center-of-momentum frame, where the center-of-mass is at rest, then the unity term in each pair of braces in Eqs. (22)–(25) vanishes. In deriving these results, we have used the values for trigonometric functions at  $\psi$ ,  $\psi/2$ , and  $\psi/4$  that are listed in Table I. We also need to evaluate the trigonometric functions at  $n\theta$ ,  $(n + \frac{1}{2})\theta$ ,  $n\psi$ ,

$(n + \frac{1}{2})\psi$ , and  $(n + \frac{1}{4})\psi$ . In Appendix D, we summarize a way to evaluate these functions in terms of  $\alpha$ .

Let us summarize properties of the solutions listed in Eqs. (22)–(25). For  $n = 0$ , the velocities satisfy the initial conditions  $a_0 = V$ ,  $b_0 = c'_0 = 0$ . As  $n$  increases,  $a_n$  decreases and  $b_n$  increases. The reason is that the impulse on  $A$  in each collision is along the  $-x$  axis and the impulse on  $B$  in each collision is along the  $+x$  axis. The terminal velocities can be obtained once we know the total numbers of collisions  $N_A$  and  $N_B$ , which are calculated in Appendix E; the results are:

$$N_A = \begin{cases} N_B = \lceil \pi/\psi \rceil - 1 & \text{for } 0 < \mathfrak{s}(\pi/\psi) \leq 1/2, \\ N_B + 1 = \lceil \pi/\psi \rceil, & \text{otherwise.} \end{cases} \quad (27)$$

Here, the ceiling function  $\lceil x \rceil$  and the sawtooth function  $\mathfrak{s}(x)$  are defined in Appendix E. Using this result, along with Eqs. (1) and (2), we find that

$$N_A = N_B = k = \frac{\pi}{\psi} - \frac{1}{2} \quad \text{if } \alpha = \alpha_k, \quad (28)$$

$$N_A - 1 = N_B = k = \frac{\pi}{\psi} - 1 \quad \text{if } \alpha = \beta_k. \quad (29)$$

At  $\alpha = 1$ ,  $\psi = 2\pi/3$  and  $N_A = N_B = 1$ . As  $\alpha$  decreases,  $\psi$  also decreases. At certain mass ratios,  $\alpha = \alpha_k - 0^+$  and  $\alpha = \beta_k - 0^+$ ,  $N_A$  and  $N_B$  increase by unity, respectively. The equalities in Eqs. (1) and (2) are determined by the step functions in Eq. (27). Note that the threshold mass ratios are ordered as  $\cdots < \beta_2 < \alpha_2 < \beta_1 < \alpha_1 = 1$ .

By making use of the analytic solutions given in Eqs. (22)–(25), we can find every pair of  $k$  and  $\psi$  that guarantee the terminal velocities satisfy the conditions  $\alpha = \alpha_k^{\text{magic}}$  and  $\alpha = \alpha_k^{\text{deficient}}$ , respectively; this verifies the existence of both  $\alpha_k^{\text{magic}}$  and  $\alpha_k^{\text{deficient}}$ . The corresponding proofs for the existence of  $\alpha_k^{\text{magic}}$  and  $\alpha_k^{\text{deficient}}$  are given in Appendices F and G, respectively.

The resultant values for the critical mass ratios can be obtained from Eqs. (20) and (28)–(29) as

$$\alpha_k^{\text{magic}} = \alpha_k = -1 + \sec\left(\frac{\pi}{2k+1}\right) \quad (30)$$

and

$$\alpha_k^{\text{deficient}} = \beta_k = -1 + \sec\left[\frac{\pi}{2(k+1)}\right], \quad (31)$$

for  $k \geq 1$ . At  $\alpha = \alpha_k^{\text{magic}}$ ,  $\psi = \pi/(k + \frac{1}{2})$  and at  $\alpha = \alpha_k^{\text{deficient}}$ ,  $\psi = \pi/(k + 1)$ . The first few values are  $\alpha_1 = 1$ ,  $\beta_1 = \sqrt{2} - 1 \approx 0.414$ ,  $\alpha_2 = \sqrt{5} - 2 \approx 0.236$ , and  $\beta_2 = (2 - \sqrt{3})/\sqrt{3} \approx 0.155$ .

In Table II, we list the ten largest values of  $\alpha_k = \alpha_k^{\text{magic}}$  and  $\beta_k = \alpha_k^{\text{deficient}}$ , and in Fig. 2, we show  $N_A$  and  $N_B$  as functions of  $\alpha$ . According to these results, both  $A$  and  $B$  will make a single collision with the ball if  $\alpha \geq 1$ , whereas if  $\sqrt{2} - 1 = \beta_1 \leq \alpha < 1$ , the ball will hit  $A$  twice and hit  $B$  only once. As previously discussed, for any  $\alpha = \alpha_k$ ,  $N_A = N_B = k$ . But  $\alpha_k$  is the minimum value of  $\alpha$  such that  $N_A = k$ . Thus, for  $\alpha$  infinitesimally smaller than  $\alpha_k$ , we have  $N_A = k + 1$  and  $N_B = k$ . Similarly, note that  $\beta_k$  is the minimum value of  $\alpha$  to have  $N_A = N_B + 1 = k + 1$ . Hence, for  $\alpha$  infinitesimally smaller than  $\beta_k$ , we have  $N_A = N_B = k + 1$ .

In Fig. 3 we show the trajectories of  $A$ ,  $B$ , and  $C$  as functions of time for (a)  $\alpha = \alpha_3 \approx 0.11$ , (b)  $\alpha = 0.12$ , and (c)  $\alpha = 0.10$ . When  $\alpha = \alpha_3$  the trajectory of  $C$  meets those of  $A$  and  $B$  three times each, consistent with  $N_A = N_B = 3$  that can be read off from Fig. 2. After  $C$  hits  $B$  three times, both  $A$  and  $C$  stop and the terminal velocity of  $B$  is the same as the initial velocity of the incident block. According to Fig. 2,  $N_A = N_B = 3$  at  $\alpha = 0.12 > \alpha_3$ , which is consistent with Fig. 3(b). At this value of  $\alpha$ , all three objects continue moving after their last collisions, and although  $C$  does not stop after its final collision with  $B$ , the terminal speeds are such that  $C$  cannot catch up with  $B$ . At  $\alpha = 0.10 < \alpha_3$ ,  $N_A = 4$  while  $N_B = 3$  according to Figs. 2 and 3(c). In this scenario,  $A$  continues to move forward after its third collision with  $C$ ; meanwhile,  $C$  moves backward after its third collision with  $B$  so that it makes another collision with  $A$ .

The terminal velocities of the two blocks can be obtained by substituting  $n = N_A$  and  $N_B$  in Eqs. (E6) and (E9) into the formulas for  $a_n$  and  $b_n$  given in Eqs. (22) and (23), to obtain

$$a_t = \frac{V}{2 + \alpha} [1 + (1 + \alpha) \cos(N_A \psi)] \quad (32)$$

and

$$b_t = \frac{V}{2 + \alpha} \{1 - (1 + \alpha) \cos[(N_B + \frac{1}{2})\psi]\}, \quad (33)$$

where we have used  $\cos(\psi/2) = (1 + \alpha)^{-1}$ . By making use of momentum conservation, we can determine the terminal velocity  $c_t$  of  $C$  as

$$c_t = \frac{V - a_t - b_t}{\alpha}, \quad (34)$$

which is the same as  $c'_{NB}$  for  $0 < \mathfrak{s}(\pi/\psi) \leq 1/2$  or  $c_{NA}$  otherwise. We can determine the terminal velocities at  $\alpha = \alpha_k$  and  $\beta_k$  by making use of Eqs. (30) and (31): when  $\alpha = \alpha_k$ , we have  $a_t = c_t = 0$  and  $b_t = V$ ; when  $\alpha = \beta_k$ , we get  $a_t = -\beta_k V/(2 + \beta_k)$  and  $b_t = c_t = 2V/(2 + \beta_k)$ .

In Fig. 4, we plot the terminal velocities  $a_t$ ,  $b_t$ , and  $c_t$  as functions of  $\alpha$ . Because the ball cannot penetrate any blocks, the three curves are ordered as  $a_t \leq c_t \leq b_t$  for all  $\alpha$ . We see that  $b_t \leq V$  for all  $\alpha$ , as expected, because  $b_t > V$  is not allowed due to energy conservation. According to the  $a_t$  curve in Fig. 4, the (terminal) recoil velocity of the incident block  $A$  is negative<sup>25</sup> for all  $\alpha \neq \alpha_k^{\text{magic}}$ .

### Inelastic collisions

Let us briefly investigate possible modifications of our predictions if the ball and the blocks do not make elastic collisions. If the collisions are not elastic, then the energy-momentum recurrence relations in Eqs. (4)–(7) are modified as

$$a_{n-1} + \alpha c'_{n-1} = a_n + \alpha c_n, \quad (35)$$

$$e(a_{n-1} - c'_{n-1}) = c_n - a_n, \quad (36)$$

$$b_{n-1} + \alpha c_n = b_n + \alpha c'_n \quad (37)$$

and

$$e(c_n - b_{n-1}) = b_n - c'_n, \quad (38)$$

where  $0 < e \leq 1$  is the coefficient of restitution between the ball and a block. (For an elastic collision  $e = 1$  and for a completely inelastic collision  $e = 0$ .) We follow the same procedure as that for the elastic case to compute the fraction of energy transmission  $\rho = b_t^2/V^2$  to the scattered block from the incident block. In Fig. 5, we show  $\rho$  as a function of  $\alpha$  for  $e = 1, 0.9, 0.8$ , and  $0.7$ . In general we see that  $\rho$  decreases as  $e$  decreases. Furthermore, this effect is magnified as  $\alpha$  decreases because the number of collisions increases. We also see that there are shifts to the right in the values of  $\alpha$  where the local maxima or minima of  $\rho$  appear. We can compare the values of  $\alpha$  with those ( $\alpha_1$ ,  $\beta_1$ ,  $\alpha_2$ , and  $\beta_2$ ) of the elastic case. At  $e = 0.9$ , for example, the shifts from  $\alpha_1$ ,  $\beta_1$ ,  $\alpha_2$ , and  $\beta_2$  are by 0 %, 0.43 %, 4.6 %, 0.84 %, respectively. The size of the shift tends to increase as  $\alpha$  decreases. For any value of  $e$ , the value of  $\alpha$  that corresponds to  $\alpha_1 = 1$  of the elastic case is invariant.

As a pedagogical example, we show a generalized version of the Newton's cradle in Fig. 6. There are five identical "blocks"  $A_k$  of mass  $M$  on a straight wire and four "balls"  $C_k$  of mass  $m_k = \alpha_k^{\text{magic}} M$  placed between each set of blocks. Initially,  $A_1$  is the only moving object and is traveling towards  $C_1$ . We assume that all collisions are elastic and neglect friction. Any two adjacent blocks  $A_k$  and  $A_{k+1}$  exchange momenta through (possibly multiple) collisions with  $C_k$  while the remainder of the system is completely at rest. After  $A_k$  makes the  $k$ th collision with  $C_k$ ,  $A_k$  stops and  $C_k$  makes the  $k$ th collision with  $A_{k+1}$ . At this point  $C_k$  stops and  $A_{k+1}$  carries the entire incident momentum of  $A_k$ . This process continues until  $A_5$  carries the initial momentum of  $A_1$ . After that,  $A_5$  bounces back against the wall to continue a similar set of multiple collisions in the opposite direction. This experiment can be carried out by making use of an air track that is typically available in undergraduate physics laboratories.

## V. CONCLUSION

We have considered the one-dimensional scattering of two identical blocks of mass  $M$  that exchange energy and momentum through elastic collisions with an intermediary ball of mass  $m = \alpha M$ . Because the ball and the target block are initially not in contact with each other, the system experiences multiple two-body collisions that are well ordered and therefore the motion of the system is uniquely determined by energy and momentum conservation.

A vector sequence  $\mathbf{V}_n$  was constructed by rescaling the velocities of the three objects in each cycle of multiple collisions. We then showed that the energy-momentum conservation laws result in transforming the vector  $\mathbf{V}_n$  through a (pure) rotation:  $\mathbf{V}_n = \Lambda^n \mathbf{V}_0$ , with  $\det[\Lambda] = +1$  and  $\mathbf{V}_n^2 = \mathbf{V}_0^2 = V^2$ . Recursive use of the covariant recurrence relation leads to analytic expressions for the velocities of the three objects after each collision. Based on these results, we have computed the total number of collisions and the terminal velocity for each object in terms of  $\alpha$ .

The covariant approach was shown to be equivalent to the billiard-ball mapping approach. While the billiard-ball mapping approach reformulates the problem into a problem of projective geometry, the covariant approach employs elementary techniques of group theory and differential geometry that are well described in standard textbooks on classical mechanics or mathematical physics. We expect that the covariant approach presented in this work can

be systematically generalized to the relativistic case.

It is rather remarkable that at magic mass ratios  $\alpha = \alpha_k^{\text{magic}}$ , the energy and momentum of the incident block are completely transferred to the target block. Such complete momentum transfer to a single scattered particle in many-body collisions is difficult to find. The only nontrivial example is Newton's cradle, which is equivalent to our model when  $\alpha = 1$ . As a pedagogical example, we have devised a generalized version of Newton's cradle (Fig. 6) that can be tested in an air track experiment.

We have also verified the identities  $\alpha_k^{\text{magic}} = \alpha_k$  and  $\alpha_k^{\text{deficient}} = \beta_k$ . In inelastic collisions, the peaks of the energy transfer fraction  $\rho$  shift from  $\alpha_k^{\text{magic}}$  and the effect increases as  $\alpha$  decreases.

## Acknowledgments

J.L. wishes to express his gratitude to the High Energy Theory Group at Argonne National Laboratory, where part of his work was carried out on a leave of absence from Korea University, for its hospitality. We thank U-Rae Kim for providing useful information on the package *animate* that enabled us to generate the animation shown in Fig. 6. This work was supported in part by Korea University. The work of J.-H.E. is supported by a Global Ph.D. Fellowship Program through the National Research Foundation of Korea funded by the Ministry of Education under Contract No. NRF-2012H1A2A1003138.

## Appendix A: Orthogonal matrices

Here, we list useful properties of orthogonal matrices in two and three dimensions that are frequently used in the text. Detailed proofs and examples can be found in standard textbooks on classical mechanics or mathematical physics, such as Refs. 23 and 24.

- If there is a linear transformation  $\mathbf{V} \rightarrow \mathbf{V}' = \mathcal{O}\mathbf{V}$  of a Euclidean vector  $\mathbf{V}$  that preserves its magnitude ( $\mathbf{V}'^2 = \mathbf{V}^2$ ), then the transformation matrix  $\mathcal{O}$  must be *orthogonal*; the inverse of  $\mathcal{O}$  is identical to its transpose:  $\mathcal{O}^{-1} = \mathcal{O}^T$ .
- The determinant of an orthogonal matrix  $\mathcal{O}$  is either +1 or -1:  $\det[\mathcal{O}] = \pm 1$ .

- A linear transformation  $\mathbf{V}' = \mathbb{P}_k \mathbf{V}$  is called a *reflection* if  $V'_i = V_i$  for all  $i \neq k$  and  $V'_k = -V_k$ . The magnitude of a vector is invariant under reflection.
- In a two-dimensional Euclidean space, any orthogonal matrix  $\mathcal{O}$  with  $\det[\mathcal{O}] = +1$  can be parametrized by  $\mathcal{O} = \lambda(\phi)$ , where  $\lambda(\phi)$  is the  $2 \times 2$  rotation matrix by angle  $\phi$ :

$$\lambda(\phi) = \begin{pmatrix} \cos \phi & -\sin \phi \\ \sin \phi & \cos \phi \end{pmatrix}. \quad (\text{A1})$$

If  $\det[\mathcal{O}] = -1$ , then  $\mathcal{O}$  can be parametrized by  $\mathcal{O} = \lambda(\phi')\mathbb{P}_2$ , which is the product of a rotation by angle  $\phi'$  and a reflection  $\mathbb{P}_2 = \text{diag}[1, -1]$ . Here,  $\text{diag}[a_1, a_2, \dots, a_n]$  stands for the diagonal matrix  $A$  whose diagonal elements are  $A_{ii} = a_i$ .

- In three dimensions, any orthogonal matrix  $\mathcal{O}$  with  $\det[\mathcal{O}] = +1$  can be parametrized by  $\mathcal{O} = \lambda_{\hat{n}}(\phi)$ , where  $\lambda_{\hat{n}}(\phi)$  is the rotation matrix about the axis parallel to a unit vector  $\hat{n}$  by angle  $\phi$ . If  $\hat{n}$  is a unit basis vector  $\hat{e}_i$  of a Cartesian coordinate system  $S$ , then we write  $\lambda_{\hat{n}}(\phi) = \lambda_i(\phi)$ , where

$$\lambda_1(\phi) = \begin{pmatrix} 1 & 0 & 0 \\ 0 & \cos \phi & -\sin \phi \\ 0 & \sin \phi & \cos \phi \end{pmatrix}, \quad (\text{A2})$$

$$\lambda_2(\phi) = \begin{pmatrix} \cos \phi & 0 & \sin \phi \\ 0 & 1 & 0 \\ -\sin \phi & 0 & \cos \phi \end{pmatrix}, \quad (\text{A3})$$

and

$$\lambda_3(\phi) = \begin{pmatrix} \cos \phi & -\sin \phi & 0 \\ \sin \phi & \cos \phi & 0 \\ 0 & 0 & 1 \end{pmatrix}. \quad (\text{A4})$$

- If the axis of rotation  $\hat{n}$  is not parallel to any axis of a Cartesian coordinate system  $S$ , then we can choose a new coordinate system  $S'$  whose triad is  $\{\hat{e}'_1, \hat{e}'_2, \hat{e}'_3 = \hat{n}\}$ . Note that the triple scalar product of the three basis vectors of a triad is  $\hat{e}_i \cdot \hat{e}_j \times \hat{e}_k = \epsilon_{ijk}$ , where  $\epsilon_{ijk}$  is the Levi-Civita tensor that is antisymmetric under exchange of any two indices and  $\epsilon_{123} = +1$ . Because the matrix representation of  $\lambda_{\hat{n}}(\phi)$  in  $S'$  is  $\lambda_3(\phi)$ , that in  $S$  can be expressed as

$$\lambda_{\hat{n}}(\phi) = R \lambda_3(\phi) R^T, \quad (\text{A5})$$

where the matrix elements of  $R$  in  $S$  are given by

$$R_{ij} = \hat{e}_i \cdot \hat{e}'_j. \quad (\text{A6})$$

It is trivial to show that  $R$  is orthogonal. If  $\det[\mathcal{O}] = -1$ , then  $\mathcal{O}$  is parametrized by  $\mathcal{O} = \lambda_{\hat{n}'}(\phi')\mathbb{P}_3$ , which is the product of a rotation about  $\hat{n}'$  by angle  $\phi'$  and a reflection  $\mathbb{P}_3 = \text{diag}[1, 1, -1]$ .

## Appendix B: Derivation of Eq. (12)

Here, we derive the recurrence relation in Eq. (12). The constraints in Eqs. (4)–(7) due to energy-momentum conservation result in

$$\begin{pmatrix} a_n \\ \sqrt{\alpha}c_n \end{pmatrix} = \Gamma \begin{pmatrix} a_{n-1} \\ \sqrt{\alpha}c'_{n-1} \end{pmatrix}, \quad (\text{B1})$$

and

$$\begin{pmatrix} b_n \\ \sqrt{\alpha}c'_n \end{pmatrix} = \Gamma \begin{pmatrix} b_{n-1} \\ \sqrt{\alpha}c_n \end{pmatrix}, \quad (\text{B2})$$

where the  $2 \times 2$  matrix  $\Gamma$  is defined by

$$\Gamma = \frac{1}{1+\alpha} \begin{pmatrix} 1-\alpha & 2\sqrt{\alpha} \\ 2\sqrt{\alpha} & -(1-\alpha) \end{pmatrix}. \quad (\text{B3})$$

According to Eqs. (5) and (7), the magnitudes of the column vectors in each of Eqs. (B1) and (B2) are invariant. Therefore,  $\Gamma$  can be parametrized by the product of a rotation matrix  $\lambda(\theta)$  and a reflection matrix  $\mathbb{P}_2$  as

$$\Gamma = \begin{pmatrix} \cos \theta & \sin \theta \\ \sin \theta & -\cos \theta \end{pmatrix} = \lambda(\theta)\mathbb{P}_2. \quad (\text{B4})$$

Because  $\det[\lambda(\theta)] = 1$  and  $\det[\mathbb{P}_2] = -1$ , we have  $\det[\Gamma] = \det[\lambda(\theta)]\det[\mathbb{P}_2] = -1$ . Here, the parameter  $\theta$  is given by

$$\theta = 2 \arctan \sqrt{\alpha}. \quad (\text{B5})$$

Because we restrict ourselves to the case  $0 < \alpha < 1$ , the range of  $\theta$  is  $0 < \theta < \pi/2$ .<sup>26</sup> (For small  $\alpha$ ,  $\theta \approx 2\sqrt{\alpha}$ .) In Table I, we list the values for trigonometric functions at  $\theta$  and  $\theta/2$ .

By making use of Eqs. (B1)–(B4), we can find the recurrence relation for the three-dimensional Euclidean-vector sequence  $\mathbf{V}_n$  of the form

$$\mathbf{V}_n = \Lambda \mathbf{V}_{n-1}. \quad (\text{B6})$$

Then  $\mathbf{V}_n$  can be expressed in terms of the initial value  $\mathbf{V}_0 = (V \ 0 \ 0)^T$  as

$$\mathbf{V}_n = \Lambda^n \mathbf{V}_0. \quad (\text{B7})$$

Next, we find the matrix representation of the matrix  $\Lambda$ . We first verify that  $\Lambda$  is a  $3 \times 3$  matrix for a pure rotation. We combine the two relations in Eqs. (B1) and (B2) to express  $\Lambda$  as

$$\Lambda = \Gamma_B \Gamma_A, \quad (\text{B8})$$

where the matrices  $\Gamma_A$  and  $\Gamma_B$  are the  $3 \times 3$  generalizations of  $\Gamma$  in Eqs. (B1) and (B2):

$$\Gamma_A = \lambda_2(-\theta) \mathbb{P}_3 = \begin{pmatrix} \cos \theta & 0 & \sin \theta \\ 0 & 1 & 0 \\ \sin \theta & 0 & -\cos \theta \end{pmatrix} \quad (\text{B9})$$

and

$$\Gamma_B = \lambda_1(\theta) \mathbb{P}_3 = \begin{pmatrix} 1 & 0 & 0 \\ 0 & \cos \theta & \sin \theta \\ 0 & \sin \theta & -\cos \theta \end{pmatrix}. \quad (\text{B10})$$

Here,  $\theta$  and  $\lambda_i(\theta)$  are defined in Eqs. (B5) and (A2)–(A4), respectively, and  $\mathbb{P}_3 = \text{diag}[1, 1, -1]$ . The explicit form of the matrix  $\Lambda$  is

$$\Lambda = \begin{pmatrix} \cos \theta & 0 & \sin \theta \\ \sin^2 \theta & \cos \theta & -\sin \theta \cos \theta \\ -\sin \theta \cos \theta & \sin \theta & \cos^2 \theta \end{pmatrix}, \quad (\text{B11})$$

which, using Table I, results in Eq. (18).

Because  $\det[\lambda_i(\theta)] = 1$  and  $\det[\mathbb{P}_3] = -1$ , we know that  $\det[\Gamma_A] = \det[\Gamma_B] = -1$  and  $\det[\Lambda] = 1$ . In addition, direct computation shows that  $\Lambda$  is orthogonal:  $\Lambda^{-1} = \Lambda^T$ . Therefore, the matrix  $\Lambda$  represents a pure rotation.

### Appendix C: Computation of $\Lambda^n$

Here, we derive the analytic expression for the matrix  $\Lambda^n$  that is necessary to compute  $\mathbf{V}_n$  in Eq. (13). Let  $\hat{n}$  and  $\psi$  be the axis and angle of rotation for the matrix  $\Lambda$ , respectively. If we choose a Cartesian coordinate system  $S'$ , in which  $\hat{n} = \hat{e}'_3$ , the matrix representation of  $\Lambda$  is of the form

$$\Lambda' = \lambda_3(\psi). \quad (\text{C1})$$

In  $S'$ ,  $\Lambda^n$  can be expressed as a single rotation:

$$(\Lambda')^n = [\lambda_3(\psi)]^n = \lambda_3(n\psi). \quad (\text{C2})$$

Then the matrices  $\Lambda$  and  $\Lambda^n$  defined in a general frame  $S$  can be expressed as

$$\Lambda = R\lambda_3(\psi)R^T \quad (\text{C3})$$

and

$$\Lambda^n = R\lambda_3(n\psi)R^T, \quad (\text{C4})$$

where the coordinate transformation matrix  $R$  is defined in Eq. (A6).

By generalizing the method in Ref. 14 for two dimensions into three dimensions, we determine the transformation matrix  $R$ . Because  $\hat{e}'_3$  is invariant under rotation  $\Lambda$ , we have

$$\Lambda\hat{e}'_3 = \hat{e}'_3. \quad (\text{C5})$$

The solution for this constraint equation is  $\hat{e}'_3 = (1 \ 1 \ \sqrt{\alpha})^T / \sqrt{2+\alpha}$ . Choosing the remaining two bases for the coordinate system  $S'$  as  $\hat{e}'_1 = \sqrt{1+(\alpha/2)} \ \hat{e}_3 \times \hat{e}'_3$  and  $\hat{e}'_2 = \hat{e}'_3 \times \hat{e}'_1$ , we determine the triad  $\{\hat{e}'_1, \hat{e}'_2, \hat{e}'_3\}$  of  $S'$ . As a result, we find that

$$R = (\hat{e}'_1 \ \hat{e}'_2 \ \hat{e}'_3) = \begin{pmatrix} -\frac{1}{\sqrt{2}} & -\sqrt{\frac{\alpha}{2(2+\alpha)}} & \frac{1}{\sqrt{2+\alpha}} \\ \frac{1}{\sqrt{2}} & -\sqrt{\frac{\alpha}{2(2+\alpha)}} & \frac{1}{\sqrt{2+\alpha}} \\ 0 & \sqrt{\frac{2}{2+\alpha}} & \frac{\sqrt{\alpha}}{\sqrt{2+\alpha}} \end{pmatrix}, \quad (\text{C6})$$

and the parameter  $\psi$  is defined by

$$\psi \equiv 2 \arctan \sqrt{\alpha(2+\alpha)}. \quad (\text{C7})$$

For  $0 < \alpha < 1$ , the range of  $\psi$  is  $0 < \psi < 2\pi/3$  (for small  $\alpha$ ,  $\psi \approx 2\sqrt{2\alpha}$ ). In Table I, we list the values for trigonometric functions at  $\psi$ ,  $\psi/2$ , and  $\psi/4$ .

## Appendix D: Special values for trigonometric functions

Here, we summarize a way to evaluate the trigonometric functions at special values such as  $n\theta$ ,  $(n + \frac{1}{2})\theta$ ,  $n\psi$ ,  $(n + \frac{1}{2})\psi$ , and  $(n + \frac{1}{4})\psi$  in terms of  $\alpha$ . The parameters  $\theta$  and  $\psi$  are defined in Eqs. (17) and (20), respectively.

### 1. At angles $nx$

We can compute  $\cos nx$  and  $\sin nx$  for  $x = \theta, \psi$  as

$$\cos nx = \Re[e^{inx}] = \sum_{k=0}^{\lfloor n/2 \rfloor} \frac{(-1)^k n!}{(2k)!(n-2k)!} \sin^{2k} x \cos^{n-2k} x \quad (\text{D1})$$

and

$$\sin nx = \Im[e^{inx}] = \sum_{k=0}^{\lfloor (n-1)/2 \rfloor} \frac{(-1)^k n!}{(2k+1)!(n-2k-1)!} \sin^{2k+1} x \cos^{n-2k-1} x, \quad (\text{D2})$$

where the floor function  $\lfloor x \rfloor$  is defined in Eq. (E2). Special values for  $\cos x$  and  $\sin x$  for  $\theta$  and  $\psi$  are given in Table I.

### 2. At angles $(n + \frac{1}{4})x$ and $(n + \frac{1}{2})x$

We can compute  $\cos(n+r)x$  and  $\sin(n+r)x$  for  $x = \theta, \psi$  and  $r = 1/2, 1/4$  as

$$\cos(n+r)x = \cos nx \cos rx - \sin nx \sin rx \quad (\text{D3})$$

and

$$\sin(n+r)x = \sin nx \cos rx + \cos nx \sin rx. \quad (\text{D4})$$

The values for  $\cos(\theta/2)$ ,  $\sin(\theta/2)$ ,  $\cos(\psi/2)$ ,  $\sin(\psi/2)$ ,  $\cos(\psi/4)$ , and  $\sin(\psi/4)$  are given in Table I.

## Appendix E: Computation of $N_A$ and $N_B$

Here, we compute the total number of collisions  $N_i$  between the ball and the block  $i$  for  $i = A$  or  $B$ . In computing  $N_A$  and  $N_B$ , it is convenient to use the ceiling ( $\lceil x \rceil$ ) and floor ( $\lfloor x \rfloor$ ) functions. For any real number  $x$  they are defined by

$$\lceil x \rceil = n \text{ satisfying } n-1 < x \leq n \quad (\text{E1})$$

and

$$\lfloor x \rfloor = n \text{ satisfying } n \leq x < n + 1, \quad (\text{E2})$$

where  $n$  is a unique integer in each case. In addition, the sawtooth function  $\mathfrak{s}(x)$  is defined by

$$\mathfrak{s}(x) = x - \lfloor x \rfloor, \quad (\text{E3})$$

where the range is  $0 \leq \mathfrak{s}(x) < 1$ .

The collision at  $P_n$  is allowed only if  $a_{n-1} > c'_{n-1}$ . After the collision at  $P_n$ , the velocities of  $A$  and  $C$  become  $a_n$  and  $c_n$ , respectively. If the ball  $C$  experiences another collision with  $B$ , then it returns to  $A$  with the velocity  $c'_n$ . If  $n = N_A$ , then  $A$ 's velocity right after  $P_n$  must be smaller than or equal to that of  $C$  right after  $Q_n$ , or

$$a_{N_A} \leq c'_{N_A}. \quad (\text{E4})$$

By making use of Eqs. (22)–(25), (E4), and Table I, we find that

$$\sin \left[ \left( N_A - \frac{1}{2} \right) \psi \right] > 0 \quad \text{and} \quad \sin \left[ \left( N_A + \frac{1}{2} \right) \psi \right] \leq 0, \quad (\text{E5})$$

with the solution of

$$N_A = \left\lceil \frac{\pi}{\psi} - \frac{1}{2} \right\rceil. \quad (\text{E6})$$

In a similar manner, we can find the constraint on  $N_B$ . The collision at  $Q_n$  is allowed only if  $c_n > b_{n-1}$ . After the collision with  $B$  at  $Q_n$ ,  $C$  makes another collision with  $A$  at  $P_{n+1}$ , resulting in the velocity  $c_{n+1}$ . Therefore, if  $n = N_B$ , we then have

$$c_{N_B+1} \leq b_{N_B}, \quad (\text{E7})$$

which leads to

$$\sin(N_B \psi) > 0 \quad \text{and} \quad \sin[(N_B + 1) \psi] \leq 0, \quad (\text{E8})$$

with the solution of

$$N_B = \left\lceil \frac{\pi}{\psi} - 1 \right\rceil. \quad (\text{E9})$$

According to Eqs. (E6) and (E9), we find that

$$N_A = \begin{cases} N_B = \lceil \pi/\psi \rceil - 1 & \text{for } 0 < \mathfrak{s}(\pi/\psi) \leq 1/2, \\ N_B + 1 = \lceil \pi/\psi \rceil, & \text{otherwise.} \end{cases} \quad (\text{E10})$$

If  $\alpha$  is small, then we can approximate Eq. (20) as  $\psi \approx 2\sqrt{2\alpha}$  to obtain

$$N_A \approx N_B \approx \frac{\pi}{2\sqrt{2\alpha}}, \quad (\text{E11})$$

which is consistent with a previous result given in Eq. (6) of Ref. 21, where the author counts the number of collisions on both sides of the ball.

### Appendix F: Proof of $\alpha_k^{\text{magic}} = \alpha_k$

Here, we verify that  $\alpha_k$  in Eq. (30) is the  $k$ th magic mass ratio  $\alpha_k^{\text{magic}}$  at which  $a_t = c_t = 0$  and  $b_t = V$ .

Verification of the largest magic mass ratio  $\alpha_1^{\text{magic}} = 1$  is trivial. In general, energy and momentum conservation requires that the condition for the magic mass ratio  $a_t = c_t = 0$  and  $b_t = V$  can be reduced into the single condition  $b_t = V$ . Applying this requirement to Eq. (33), we find that

$$\cos[(N_B + \frac{1}{2})\psi] = -1. \quad (\text{F1})$$

Because the contact force on the block  $B$  due to the collision with  $C$  is always along the positive  $x$ -axis, the acceleration of  $B$  is never negative. Therefore,  $b_t$  in Eq. (33) is never decreasing, which requires that

$$N_B = \frac{\pi}{\psi} - \frac{1}{2}. \quad (\text{F2})$$

If we substitute the value for  $\psi$  into Eq. (20), then the constraint is equivalent to a quadratic equation, whose unique solution is given by Eq. (30).

### Appendix G: Proof of $\alpha_k^{\text{deficient}} = \beta_k$

In this appendix, we verify that  $\beta_k$  defined in Eq. (31) is identical to the deficient mass ratio  $\alpha_k^{\text{deficient}}$  at which  $b_t$  reaches the local minimum within the region  $\alpha_{k+1} < \alpha < \alpha_k$ .

As shown in Fig. 4, the terminal velocity  $b_t$  has local minima. At each local minimum, the ball is at a local maximum and  $b_t = c_t$ . Next, we verify the statement that  $b_t = c_t$  at  $\alpha = \beta_k$  for any  $k \geq 1$ . If we require  $b_t = c_t$ , then conservation of energy and momentum lead to

$$(1 + \alpha)b_t + a_t = V \quad (\text{G1})$$

and

$$(1 + \alpha)b_t^2 + a_t^2 = V^2. \quad (\text{G2})$$

These coupled quadratic equations have a trivial solution  $b_t = 0$  and  $a_t = V$  that is equivalent to the initial condition. Because the three objects do not penetrate each other, we discard this trivial solution. Then we have a unique set of solutions:

$$a_t = -\frac{\alpha V}{2 + \alpha} \quad (\text{G3})$$

and

$$b_t = \frac{2V}{2 + \alpha}. \quad (\text{G4})$$

By comparing Eq. (33) and Eq. (G4), we find that

$$\cos[(N_B + \frac{1}{2})\psi] = -\frac{1}{1 + \alpha}, \quad (\text{G5})$$

with a solution of

$$N_B = \frac{\pi}{\psi} - 1, \quad (\text{G6})$$

which is equivalent to Eq. (31) with the value for  $\psi$  in Eq. (20).

---

\* Electronic address: jungil@korea.ac.kr

<sup>1</sup> Let us denote by  $u_i$  and  $v_i$  the initial and final velocities of the  $i$ th object, respectively. Then conservation of energy and momentum require  $u_1 + u_2 = v_1 + v_2$  and  $u_1^2 + u_2^2 = v_1^2 + v_2^2$ . These coupled equations have a unique set of solutions:  $v_1 = u_2$  and  $v_2 = u_1$ . If they do not make a collision, then  $v_1 = u_1$  and  $v_2 = u_2$ .

<sup>2</sup> J. B. Hart and R. B. Herrmann, “Energy transfer in one-dimensional collisions of many objects,” Am. J. Phys. **36**, 46–49 (1968).

<sup>3</sup> J. D. Kerwin, “Velocity, momentum, and energy transmissions in chain collisions,” Am. J. Phys. **40**, 1152–1157 (1972).

<sup>4</sup> J. D. Gavenda and J. R. Edgington, “Newton’s cradle and scientific explanation,” Phys. Teach. **35**, 411–417 (1997).

<sup>5</sup> S. Chapman, “Misconception concerning the dynamics of the impact ball apparatus,” Am. J. Phys. **28**, 705–711 (1960).

- <sup>6</sup> L. Flansburg and K. Hudnut, “Dynamic solutions for linear elastic collisions,” Am. J. Phys. **47**, 911–914 (1979).
- <sup>7</sup> F. Herrmann and P. Schmälzle, “Simple explanation of a well-known collision experiment,” Am. J. Phys. **49**, 761–764 (1981).
- <sup>8</sup> F. Herrmann and M. Seitz, “How does the ball-chain work?,” Am. J. Phys. **50**, 977–981 (1982).
- <sup>9</sup> B. Leroy “Collision between two balls accompanied by deformation: A qualitative approach to Hertz’s theory,” Am. J. Phys. **53**, 346–349 (1985).
- <sup>10</sup> P. Patricío, “The Hertz contact in chain elastic collisions,” Am. J. Phys. **72**, 1488–1491 (2004).
- <sup>11</sup> R. Hessel, A. C. Perinotto, R. A. M. Alfaro, and A. A. Freschi, “Force-versus-time curves during collisions between two identical steel balls,” Am. J. Phys. **74**, 176–179 (2006).
- <sup>12</sup> R. Cross, “Vertical bounce of two vertically aligned balls,” Am. J. Phys. **75**, 1009–1016 (2007).
- <sup>13</sup> R. Cross, “Difference between bouncing balls, springs, and rods,” Am. J. Phys. **76**, 908–915 (2008).
- <sup>14</sup> J.-H. Ee and J. Lee, “A unique pure mechanical system revealing dipole repulsion,” Am. J. Phys. **80**, 1078–1084 (2012).
- <sup>15</sup> S. De, “Derivation of an inverse square force from a gedanken construction,” Physics and Technology Quest, **2**, 35–37 (1997).
- <sup>16</sup> Y. G. Sinai, “Dynamics of a heavy particle surrounded by a finite number of light particles,” Theor. Math. Phys. **121**, 1351–1357 (1999).
- <sup>17</sup> Y. G. Sinai, *Introduction to ergodic theory*, (Princeton University Press, Princeton, 1979), 1st ed.
- <sup>18</sup> V. V. Kozlov and D. V. Treshchev, *Billiards: A genetic introduction to the dynamics of systems with impacts*, (American Mathematical Society, Providence, 1991), 1st ed.
- <sup>19</sup> S. Tabachnikov, *Billiards*, (Societe Mathematique De France, Paris, 1995), 1st ed.
- <sup>20</sup> E. Gutkin, “Billiards in polygons: survey of recent results,” J. Stat. Phys. **83**, 7–26 (1996).
- <sup>21</sup> S. Redner, “A billiard-theoretic approach to elementary one-dimensional elastic collisions,” Am. J. Phys. **72**, 1492–1498 (2004).
- <sup>22</sup> Let us consider the last collision between  $C$  and  $B$  at  $Q_k$  when  $\alpha = \alpha_k^{\text{magic}}$ . At  $Q_k$  the velocity of  $C$  changes from  $v$  to 0 and that of  $B$  changes from  $V'$  to  $V$ . Energy-momentum conservation requires  $\alpha v + V' = V$  and  $\alpha v^2 + V'^2 = V^2$ . The solutions to  $v$  and  $V'$  are  $v = 2V/(1 + \alpha)$  and  $V' = V(1 - \alpha)/(1 + \alpha)$ . In a similar manner, we find that the velocities of  $A$  and  $C$  must

be  $4\alpha V/(1+\alpha)^2$  and  $-2V(1-\alpha)/(1+\alpha)^2$ , respectively, just before the collision at  $P_k$ . This guarantees that  $A$  stops at  $P_k$  and  $C$  moves with the velocity  $v = 2V/(1+\alpha)$  between  $P_k$  and  $Q_k$ .

<sup>23</sup> S. T. Thornton and J. B. Marion, *Classical Dynamics of Particles and Systems*, (Brooks/Cole, Belmont, 2004), 5th ed.

<sup>24</sup> G. B. Arfken and H. J. Weber, *Mathematical Methods for Physicists*, (Elsevier, Boston, 2005), 6th ed.

<sup>25</sup> We can show that  $-\alpha V/(2+\alpha) \leq a_t \leq 0$  by making use of Eq. (32) and the constraint  $\pi - (\psi/2) \leq N_A < \pi + (\psi/2)$  that derives from Eq. (E6).

<sup>26</sup> Note that  $\alpha = 0$  represents the case that the ball is absent.

## Tables

TABLE I: The values of  $\cos x$ ,  $\sin x$ , and  $\tan x$  at  $x = \theta/2$ ,  $\theta$ ,  $\psi/4$ ,  $\psi/2$ , and  $\psi$  as functions of  $\alpha$ , where  $\theta = 2 \arctan \sqrt{\alpha}$  and  $\psi = 2 \arctan \sqrt{\alpha(2 + \alpha)}$ .

$x \setminus f(x)$	$\cos x$	$\sin x$	$\tan x$
$\frac{\theta}{2}$	$\frac{1}{\sqrt{1+\alpha}}$	$\sqrt{\frac{\alpha}{1+\alpha}}$	$\sqrt{\alpha}$
$\theta$	$\frac{1-\alpha}{1+\alpha}$	$\frac{2\sqrt{\alpha}}{1+\alpha}$	$\frac{2\sqrt{\alpha}}{1-\alpha}$
$\frac{\psi}{4}$	$\sqrt{\frac{2+\alpha}{2(1+\alpha)}}$	$\sqrt{\frac{\alpha}{2(1+\alpha)}}$	$\sqrt{\frac{\alpha}{2+\alpha}}$
$\frac{\psi}{2}$	$\frac{1}{1+\alpha}$	$\frac{\sqrt{\alpha(2+\alpha)}}{1+\alpha}$	$\sqrt{\alpha(2+\alpha)}$
$\psi$	$\frac{1-2\alpha-\alpha^2}{(1+\alpha)^2}$	$\frac{2\sqrt{\alpha(2+\alpha)}}{(1+\alpha)^2}$	$\frac{2\sqrt{\alpha(2+\alpha)}}{1-2\alpha-\alpha^2}$

TABLE II: The ten largest values for the magic mass ratio  $\alpha_k^{\text{magic}}$  and the deficient mass ratio  $\alpha_k^{\text{deficient}}$  that are defined in Eqs. (30) and (31). The proofs of the relations with threshold mass ratios  $\alpha_k^{\text{magic}} = \alpha_k$  and  $\alpha_k^{\text{deficient}} = \beta_k$  are given in Appendices F and G, respectively.

$k$	$\alpha_k^{\text{magic}} = \alpha_k$	$\alpha_k^{\text{deficient}} = \beta_k$
1	1	0.414214
2	0.236068	0.154701
3	0.109916	0.082392
4	0.064178	0.051462
5	0.042217	0.035276
6	0.029927	0.025717
7	0.022341	0.019591
8	0.017321	0.015427
9	0.013827	0.012465
10	0.011295	0.010283

## Figure Captions

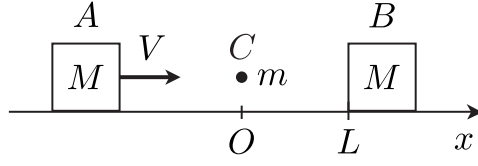


FIG. 1: The initial condition of the model system. Block  $A$  with initial speed  $V$  is approaching ball  $C$  and block  $B$  that are at rest at  $x = 0$  and  $L$ , respectively. Both blocks have mass  $M$  and  $m = \alpha M$  is the mass of the ball, with  $\alpha < 1$ .

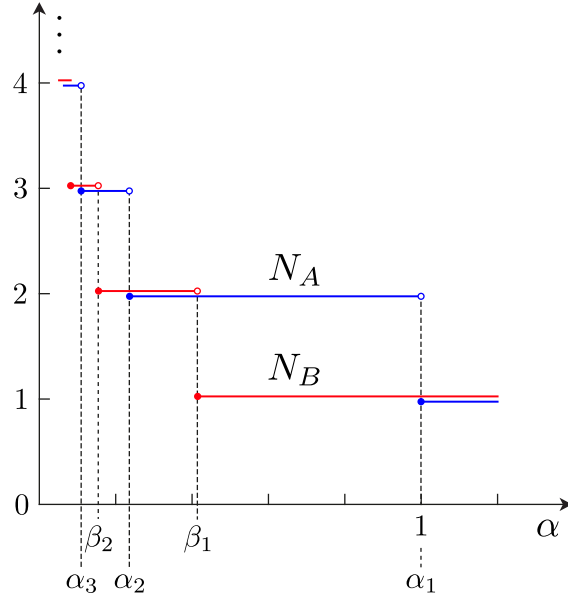


FIG. 2: The number of collisions  $N_A$  and  $N_B$  as functions of  $\alpha$ . The threshold mass ratios  $\alpha_k$  and  $\beta_k$  are the minimum values of  $\alpha$  to have  $N_A = N_B = k$ , respectively, for  $k \geq 1$ .

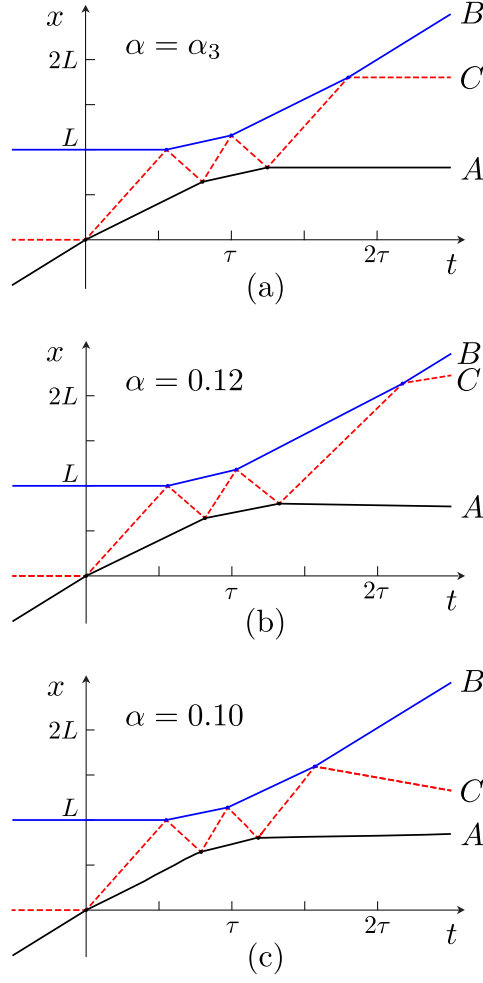


FIG. 3: The trajectories of  $A$ ,  $B$ , and  $C$  as functions of time for: (a)  $\alpha = \alpha_3^{\text{magic}} \approx 0.11$ , (b)  $\alpha = 0.12$ , and (c)  $\alpha = 0.10$ , where  $\tau \equiv L/V$ . The lower and upper lines represent the trajectories of  $A$  and  $B$ , respectively, and the dashed line is for  $C$ . At  $\alpha = \alpha_3^{\text{magic}}$  [panel (a)], the scattered block carries the total initial momentum of the incident block.

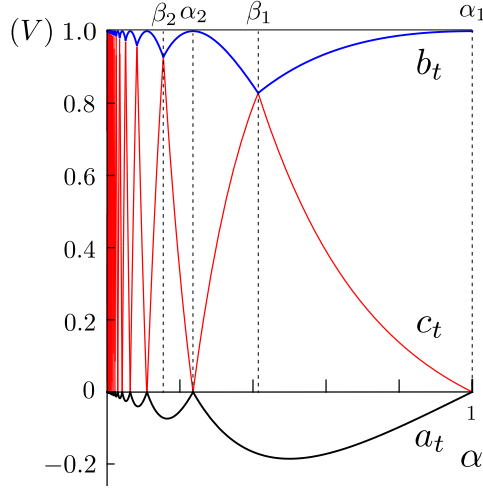


FIG. 4: The terminal velocities  $a_t$ ,  $b_t$ , and  $c_t$  of  $A$ ,  $B$ , and  $C$ , respectively, in units of the initial velocity  $V$  of  $A$  as functions of the mass ratio  $\alpha$ . At every  $\alpha = \alpha_k$ , we have  $b_t = V$  and  $a_t = c_t = 0$  for  $k \geq 1$ . At every  $\alpha = \beta_k$ , we have  $b_t = c_t$ , and  $b_t$  becomes a local minimum for  $k \geq 1$ .

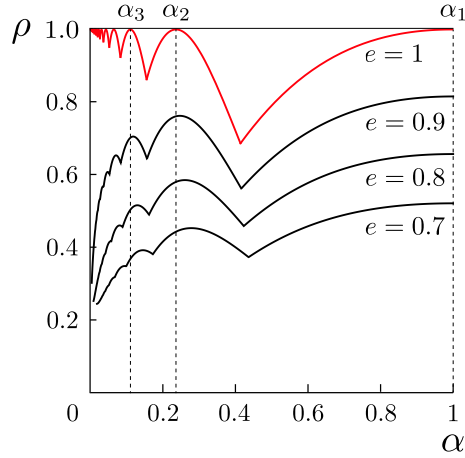


FIG. 5: The fraction  $\rho = b_t^2/V^2$  of energy transmission to the target block as a function of  $\alpha$  for different coefficients of restitution  $e$ .

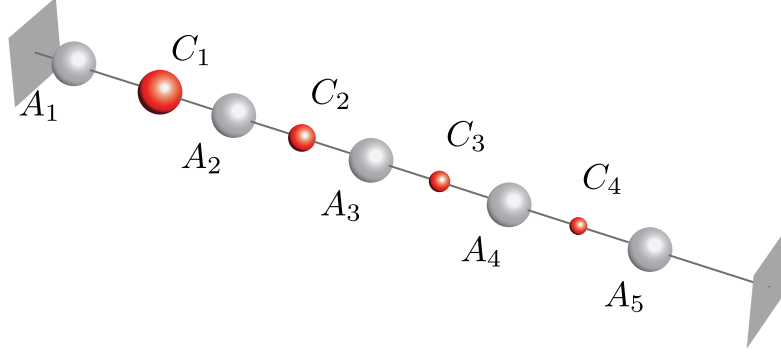


FIG. 6: A generalized version of Newton's cradle consisting of beads on a horizontal frictionless straight wire. There are five identical "blocks"  $A_k$  of mass  $M$  on a straight wire and a "ball"  $C_k$  of mass  $m_k = \alpha_k^{\text{magic}} M$  between each set of blocks. Initially, all blocks are at rest except  $A_1$ , which is moving towards  $C_1$ . After  $A_k$  makes the  $k$ th collision with  $C_k$ ,  $A_k$  stops and  $C_k$  makes the  $k$ th collision with  $A_{k+1}$ . Then  $C_k$  stops and  $A_{k+1}$  carries the complete amount of the incident momentum of  $A_k$ . This process continues until  $A_5$  carries the initial momentum of  $A_1$ . After that,  $A_5$  bounces back against the wall and the process repeats in the reverse direction. (Enhanced online) [URL: <http://dx.doi.org/10.1119/1.4897162.1>]